Biochemical and Biophysical Research Communications 454 (2014) 404–409

Contents lists available at ScienceDirect

Biochemical and Biophysical Research Communications

journal homepage: www.elsevier.com/locate/ybbrc

Interaction between S100P and the anti-allergy drug cromolyn

Srinivasa R. Penumutchu [a], Ruey-Hwang Chou [b,c], Chin Yu [a,d,*]

[a] Department of Chemistry, National Tsing Hua University, Hsinchu 30013, Taiwan
[b] Graduate Institute of Cancer Biology and Center for Molecular Medicine, China Medical University, Taichung 404, Taiwan
[c] Department of Biotechnology, Asia University, Taichung 413, Taiwan
[d] The Key Laboratory for Chemical Biology of Fujian Province, College of Chemistry and Chemical Engineering, Xiamen University, Xiamen 361005, China

ARTICLE INFO

Article history:
Received 3 October 2014
Available online 17 October 2014

Keywords:
S100P protein
Cromolyn
HSQC
HADDOCK
Molecular dynamics

ABSTRACT

The S100P protein has been known to mediate cell proliferation by binding the receptor for advanced glycation end products (RAGE) to activate signaling pathways, such as the extracellular regulated kinase (ERK) and nuclear factor kappa-light-chain-enhancer of activated B cells (NF-κB) pathways. S100P/RAGE signaling is involved in a variety of diseases, such as cancer, metastasis, and diabetes. Cromolyn is an anti-allergy drug that binds S100P to block the interaction between S100P and RAGE. In the present study, we characterized the properties of the binding between cromolyn and calcium-bound S100P using various biophysical techniques. The binding affinity for S100P and cromolyn was measured to be in the millimolar range by fluorescence spectroscopy. NMR-HSQC titration experiments and HADDOCK modeling was employed to determine the spatial structure of the proposed heterotetramer model of the S100P–cromolyn complex. Additional MD simulation results revealed the important properties in the complex stability and conformational flexibility of the S100P–cromolyn complex. This proposed model has provided an understanding of the molecular level interactions of S100P–cromolyn complex.

© 2014 Elsevier Inc. All rights reserved.

1. Introduction

The S100 proteins are calcium-binding EF-hand proteins. The calcium-induced conformational change in S100 proteins results in exposure of the hydrophobic surface between a loop region (between helix-2 and helix-3) and either helix-4 or the subsequent C-terminus to bind protein targets and regulate biological functions [1,2]. These S100 proteins are known to be expressed in a tissue-specific and cell-specific pattern. Importantly, S100 proteins influence different functions both extracellularly and intracellularly by direct interaction with specific target proteins. Misregulation of these interactions is observed in a wide range of pathologies, thus making S100 proteins potential drug targets [3,4]. For instance, the S100P protein is over-expressed in pancreatic, breast, lung and colon cancer cells and regulates biological function upon binding to RAGE extracellularly [5]. Thus, it is used as a clinical marker of various cancers. The direct interaction between S100P and RAGE has been confirmed by co-immunoprecipitation and activation of downstream signaling pathways, such as the extracellular regulated kinases (ERK) and nuclear factor kappa-light-chain-enhancer of activated B cell (NF-κB) pathways [6,7]. Therefore, elevated levels of S100P can activate the downstream pathways, including the mitogen-activated protein (MAP) kinase, ERK and NF-κB pathways, and are associated with the tumor growth in various types of cancer [7–10].

Cromolyn is used to treat various diseases, including allergic rhinitis, allergic conjunctivitis, and mastocytosis [11–13]. Previous studies using affinity chromatography reported that S100P binds to cromolyn and blocks the interaction between S100P and RAGE, leading to inhibition of S100P-stimulated cell growth, invasion, and NF-κB activity in S100P-expressing BxPC-3 and MPanc-96 pancreatic cancer cells, but not in Panc-1 cells without endogenous S100P [14]. Recently, cromolyn analogs were reported to block the interaction between S100P and RAGE [15]. In the current study, we aimed to map the binding interface of S100P for cromolyn and characterized the model structure of S100P–cromolyn. Overall, the results provide significant insights into S100P–RAGE interactions.

2. Materials and methods

2.1. Reagents and chemicals

$^{15}NH_4Cl$ and D_2O were obtained from Cambridge Isotope Laboratories. Luria Broth was obtained from AMRESCO. Cromolyn

* Corresponding author at: Department of Chemistry, National Tsing Hua University, Hsinchu 30013, Taiwan. Fax: +886 35 711082.
E-mail address: cyu.nthu@gmail.com (C. Yu).

http://dx.doi.org/10.1016/j.bbrc.2014.10.048
0006-291X/© 2014 Elsevier Inc. All rights reserved.

was purchased from Sigma–Aldrich. All used chemicals were analytical grade.

2.2. Expression and purification of S100P

Recombinant wild-type S100P (95 amino acids) was cloned into the pET-20b (+) T7 expression vector, over-expressed in the *Escherichia coli* BL21 (DE3) strain and purified using a previously reported procedure [16]. The S100P protein was eluted as a dimer from a Superdex-75 column (1.6 × 60 cm; Pharmacia). The purity was estimated to be 95% by SDS–PAGE separation, and the molecular weight was confirmed by electrospray ionization (ESI) mass spectrometry.

2.3. Fluorescence experiments

The fluorescence experiments were conducted using a Hitachi F-2500 fluorescence spectrophotometer. Cromolyn exhibits a broad absorption band at the wavelength of 326 nm, and the emission maximum was observed in the range from 400 to 600 nm. The changes in the emission spectra were monitored by increasing the concentration of S100P (0 μM, 12 μM, 24 μM, 28 μM, 32 μM, 40 μM, 44 μM, 48 μM, 52 μM, 56 μM, 60 μM, 80 μM, 100 μM, 120 μM, 130 μM, 160 μM and 170 μM) in the mixture with cromolyn (concentration of probe = 34 μM). The extent of cromolyn binding to the S100P protein was determined using the Benesi Hildebrand relation [17,18]. The data were plotted as 1/[S100P] versus $1/I - I_0$, and linear curve fitting in the Origin program was used to calculate the extent of binding using the following equation.

$$1/(I - I_0) = 1/(I_1 - I_0) + 1/(I_1 - I_0)\ K\ [\text{S100P}] \quad (1)$$

where I_0, I and I_1 represent the emission intensities in the absence of, at an intermediate concentration of and at an infinite concentration of cromolyn, and K indicates the extent of binding.

2.4. NMR HSQC titration experiments

The HSQC NMR data were collected at 25 °C with a Varian 700 NMR spectrometer with cryogenic probes. The backbone chemical shift assignment of the calcium-bound S100P was used as previously described for the same buffer [16]. Cromolyn was added to the uniformly labeled ^{15}N-S100P protein at different molar ratios, including 1:0.33, 1:0.66, 1:1, 1:2, 1:3, and 1:4. All of the spectra were processed with VnmrJ 2.3 and analyzed with SPARKY.

2.5. Molecular docking

High ambiguity driven protein–protein docking (HADDOCK) was used to dock S100P and cromolyn and to obtain the tetrameric S100P–cromolyn complex [19,20]. The structural coordinates for the calcium-bound S100P were taken from the Protein Data Bank as input data (PDB ID:1J55) [21]. The three-dimensional coordinates of cromolyn have been taken from Cambridge Structural Database center (CSDC:1022446). The residues with significantly perturbed NMR chemical shifts were defined as ambiguous interaction restraints for the residues at the interface of the S100P protein. The active and passive residues were defined using NACCESS [22]. The relative residue accessible surface area larger than 30% for either side chain or backbone atoms was defined as the active residues and the relative residue accessible surface area less than 30% for either side chain or backbone atoms was defined as passive residues. The 2000 total structures from the rigid body docking were employed using the standard HADDOCK protocol with optimized potential for liquid simulations (OPLSX) parameters [23]. The 200 lowest energy structures were used for subsequent semi-flexible simulated annealing and explicit solvent refinement to optimize the side-chain contacts. PyMOL was used for structural representations.

2.6. Molecular dynamics (MD) simulations

The MD simulations of S100P–cromolyn were performed using GROMACS 4.5.5 [24,25] with the GROMOS 53a6 force field. The lowest energy structure of the HADDOCK-modeled S100P–cromolyn complex was selected for further MD simulation study. The topology parameters of S100P were generated using the GROMACS program. The topology parameters of cromolyn were created using the ATB server for GROMOS force fields [26]. The free S100P protein and S100P–cromolyn complex were solvated with explicit SPC water system molecules in a cubic box. Sodium and chloride ions were added to neutralize the systems. Van der Waals interactions were modeled using 6–12 Lennard-Jones potentials with a 1.4 nm cutoff. Long-range electrostatic interactions were calculated using the particle mesh Ewald method. Covalent bonds were constrained by the LINCS algorithm. Each system was simulated with 100 ps of energy minimization for 50,000 iterations at constant temperature and pressure. For this NPT simulation structure, the production run for simulation was performed for 15 ns without restraint for each system. The coordinates were saved every 2 ps using a time step of 2 fs to analyze the MD trajectories. Additional

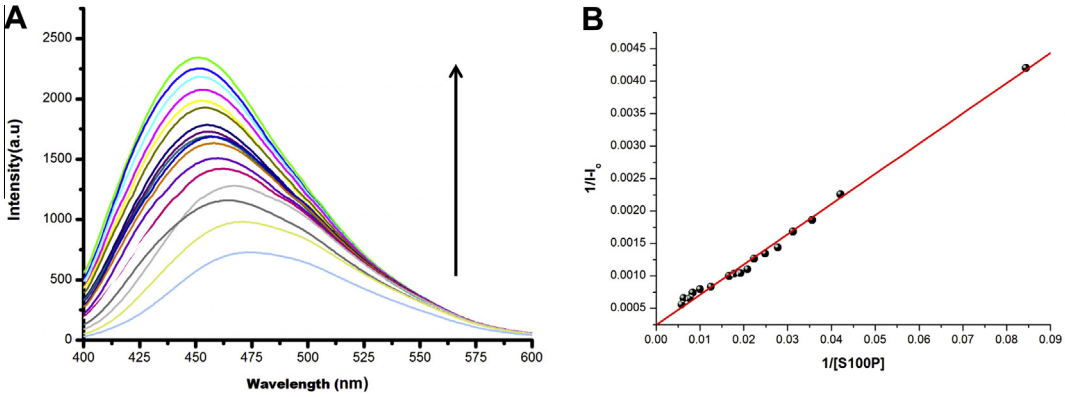

Fig. 1. (A) Changes in the fluorescence spectra of cromolyn (concentration of probe = 34 μM) with increasing concentrations of the S100P protein (0 μM, 12 μM, 24 μM, 28 μM, 32 μM, 40 μM, 44 μM, 48 μM, 52 μM, 56 μM, 60 μM, 80 μM, 100 μM, 120 μM, 130 μM, 160 μM and 170 μM). (B) Benesi–Hildebrand plot of $1/[I - I_0]$ versus 1/[protein] (M^{-1}) for the binding of cromolyn to S100P.

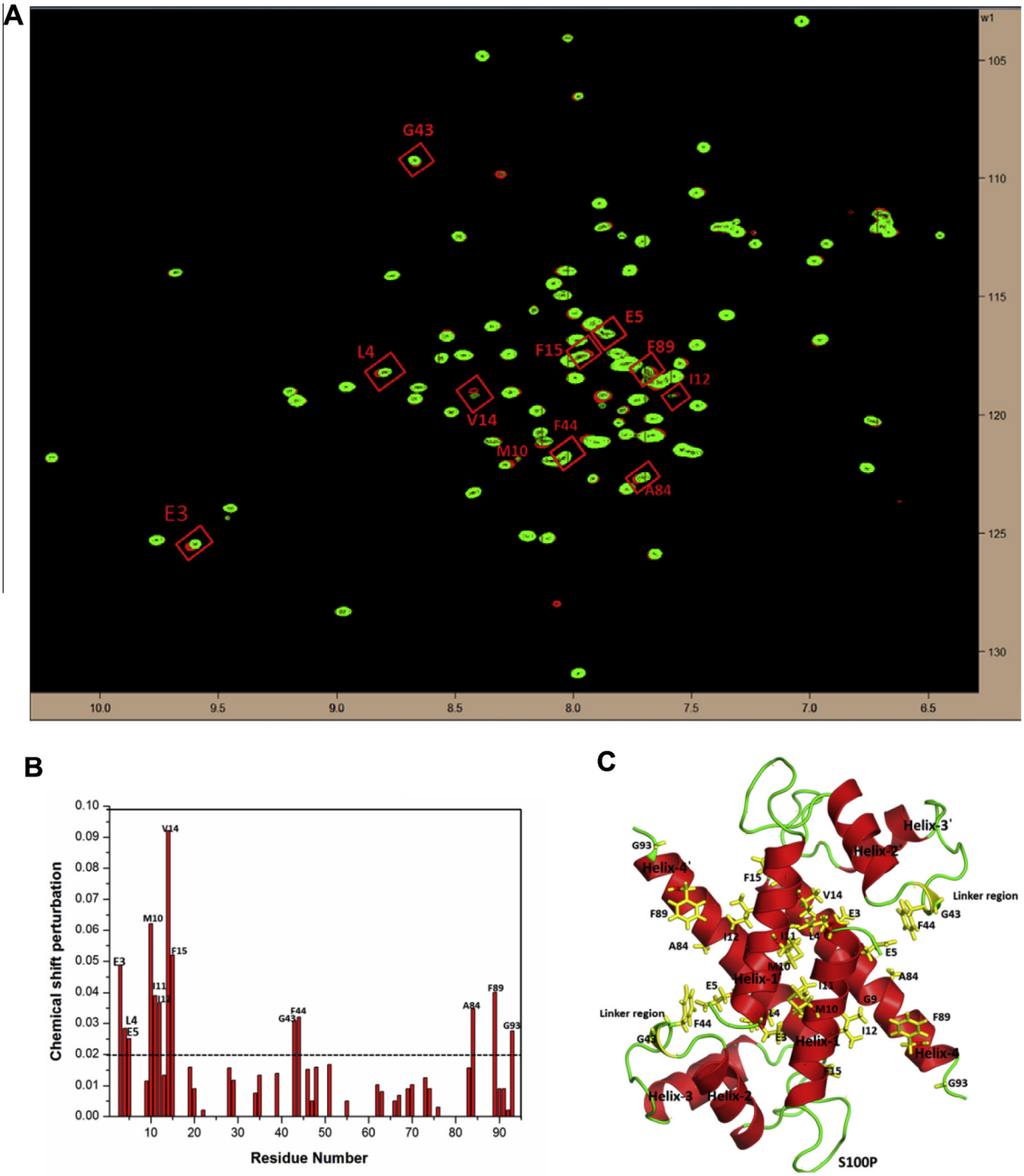

Fig. 2. (A) Overlay of the ^{15}N-^{1}H HSQC spectra of free 0.3 mM ^{15}N-labeled S100P (red) and in the complex form with 1.2 mM of the cromolyn (green), are shown. (B) Bar diagram of the weighted average of the chemical shift (^{1}H and ^{15}N) variations $\Delta\delta = [(\delta^{1}HN)^2 + 0.2\ (\delta^{15}N)^2]^{1/2}$ of the amino acid residues in the S100P–cromolyn adduct. The black dashed line indicates the selected residues that exhibited a significant chemical shift perturbation ($\Delta\delta > 0.02$ ppm). (C) Cartoon-stick representations of the S100P–cromolyn interactions; the residues with significantly perturbed chemical shifts are shown in yellow for both S100P subunits. (For interpretation of the references to color in this figure legend, the reader is referred to the web version of this article.)

GROMACS tools were used for the analysis. The VMD 1.9.1 package was employed to visualize the trajectories and represent the structures [27].

3. Results and discussion

3.1. Fluorescence spectroscopy studies of S100P–cromolyn interactions

The cromolyn molecule showed two distinct UV absorption bands at ~265 nm and ~326 nm (Fig. S-1). The 326 nm absorption band of cromolyn was selected for this study. Upon excitation at 326 nm, changes in the emission of cromolyn were observed in the range from 400 to 600 nm. As shown in Fig. 1A, the addition of S100P to a 34 μM solution of cromolyn in 20 mM Tris buffer, pH = 7.5, 100 mM KCl, and 4 mM $CaCl_2$ resulted in both a gradual shift in the emission maxima and a blue shift in the lower energy charge-transfer (CT) band from ~475 nm to ~450 nm in the presence of 170 μM of S100P. The blue shift of the emission maxima of the CT band indicated that the probe molecule was encapsulated inside the hydrophobic cavity of the S100P protein. Further plotting of $1/[I - I_0]$ versus 1/[S100P] for the Benesi–Hildebrand

relation showed a linear relationship, indicating the formation of 1:1 complex between S100P and cromolyn (Fig. 1B). The 1:1 stoichiometry of the binding interaction indicated the existence of the two identical binding sites between two cromolyn molecules and the S100P dimer. The extent of binding was calculated from the ratio between the intercept and the slope of Benesi–Hildebrand plot. The calculated dissociation constant was in the millimolar range (~0.181 μM). The calculated binding constant was consistent with the previous NMR-derived K_d results for the S100A13-cromolyn interaction [28].

3.2. NMR characterization of the binding interface between cromolyn and S100P

The NMR ^{15}N-^{1}H HSQC experiment is a useful technique to identify ligand-binding sites on proteins. The ligand-binding interface on a protein can be mapped as a perturbation of the chemical shifts of the cross peaks in ^{15}N-^{1}H HSQC spectra of free protein and of the ligand–protein complex. Thus, a set of ^{15}N-^{1}H HSQC titrations was employed to map the binding interface between S100P and cromolyn. Upon the binding of S100P to cromolyn, changes in the ^{15}N-^{1}H backbone resonance of S100P were observed relative to that of the free protein spectra. However, analysis of the residues with perturbed chemical shifts revealed that the hydrophobic binding interface comprised the linker region, helix-4 of one S100P subunit and helix-1 of the other S100P subunit of the dimer. The residues with significantly perturbed chemical shifts were E3, L4, E5, M10, I11, I12, V14 and F15 from Helix-1; G43 and F44 from the linker region; and A84, F89 and G93 from the Helix-4 region, as shown in Fig. 2A and B. Mapping these residues on the S100 dimer revealed the existence of the two symmetrical hydrophobic interfaces for cromolyn binding on either side of the S100P dimer (Fig. 2C).

3.3. Modeling of the S100P–cromolyn complex

HADDOCK was employed using NMR-derived restraints to model the S100P–cromolyn complex. Ambiguous interaction restraints (AIRs) were derived from the residues with significantly perturbed chemical shifts in the ^{15}N-^{1}H HSQC titration experiment. The active and passive residues for the HADDOCK calculations are tabulated in Supplementary Table 1. The minimal structural change in the ^{15}N-^{1}H HSQC backbone indicated that there was no major conformational change in S100P upon forming a complex with cromolyn. Furthermore, the HADDOCK approach was used to obtain the lowest energy structures of the S100P–cromolyn complex. In total, 200 structures of solvent refinement from HADDOCK were divided into five clusters. The lowest energy conformations of clusters was selected for further analysis (Fig. 3A). The cromolyn molecule moiety was located within the hydrophobic pocket of S100P. The phenyl rings of cromolyn interacted with F89, C85, F44 and I81 of the S100P protein. Furthermore, the specific hydrogen bond was between the hydroxyl group of cromolyn and E5 of the S100P protein. Therefore, the molecular docking results indicated that the interaction between cromolyn and S100P is dominated by hydrophobic interactions (Fig. 3B), which is in agreement with the results obtained from the fluorescence experiments. PROCHECK analysis of the S100P–cromolyn complex indicated good stereochemistry for the bond angles and bond lengths and showed that 99.4% of all non-glycine residues fell within the allowed region of the Ramachandran plot, as shown by the tabulated docking statistics (Fig. S-2).

3.4. Molecular dynamics simulations of the S100P–cromolyn complex

MD simulation is a useful technique to assess conformational flexibility and complex stability and to optimize contacts at the molecular level. The modeled HADDOCK complex of S100P–cromolyn and the crystal structure of calcium-bound S100P were employed for a 15 ns MD simulation, as shown in (Fig. S-3). The root mean square deviation (RMSD) values of the backbone atoms of S100P and S100P in its complex with cromolyn relative to corresponding starting structures were calculated, as shown in Fig. 4A. The resulting RMSD values for the backbone atoms reached equilibration after 3 ns and 1 ns for the free S100P and the S100P–cromolyn complex, respectively. The positional RMSD of cromolyn was also plotted from the corresponding starting structures. The positional RMSD of cromolyn was stabilized within 1 ns, and,

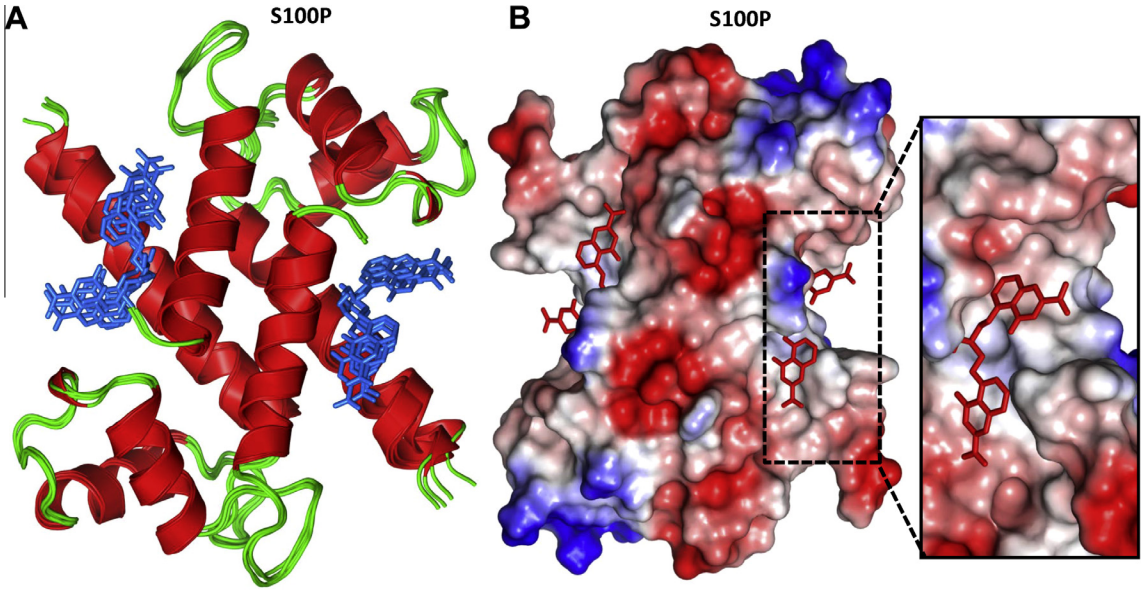

Fig. 3. HADDOCK structure of the S100P–cromolyn complex. (A) Ribbon-stick representation of the overlap of four S100P–cromolyn complex structures. Cromolyn is shown in blue, the secondary structure elements of the S100P homodimer colored red and green. (B) Electrostatic surface representation of the S100P–cromolyn complex. Cromolyn was displayed in red. The positively charged, negatively charged, and neutral amino acid residue surfaces are represented in blue, red and white, respectively. (For interpretation of the references to color in this figure legend, the reader is referred to the web version of this article.)

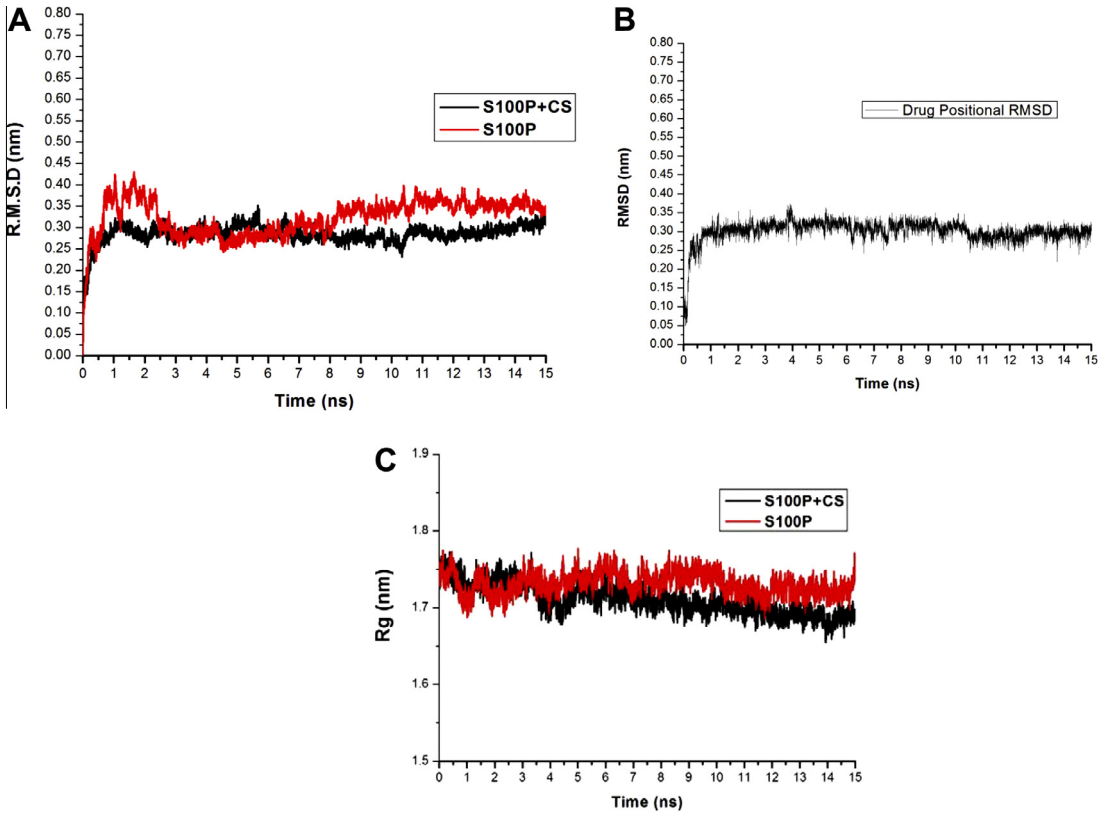

Fig. 4. Molecular dynamics simulation study of the S100P–cromolyn complex. (A) Backbone RMSD plot of the S100P protein, both free and in complex with cromolyn, during the 15 ns molecular dynamics (MD) simulation. (B) Positional RMSD of cromolyn within the binding pocket of the S100P protein. (C) Radius of gyration, Rg, during the 15 ns MD simulation of S100P and cromolyn.

furthermore, it was stable during the 15 ns simulation, as shown in Fig. 4B. In the present study, the initial radius of gyration of the free S100P protein and S100P complexed with cromolyn was 1.75 nm. In the both systems, the free S100P protein and the S100P–cromolyn complex were further stabilized at 1.73 ± 0.03 nm and 1.72 ± 0.04 nm, respectively, along the entire trajectory (15 ns), as shown in Fig. 4C. The two systems had a very similar radius of gyration, indicating that there is no major global conformational change of S100P upon the formation of a complex with cromolyn. Furthermore, analysis of the circular dichroism (CD) spectra of wild-type S100P and S100P–cromolyn showed no significant changes in the secondary structure of S100P upon the formation of a complex with cromolyn (Fig. S-4).

3.5. Description of the binding interface between S100P and cromolyn

Previous studies have shown that cromolyn binds to S100P and blocks the interaction with RAGE, thereby reducing the tumor growth and invasion of pancreatic cancer in a mouse model [14]. Disrupting the formation of the S100P–RAGE complex is an effective strategy to prevent various cancers. Recently, the structural characterization of the S100P–RAGE V binary complex (PDB ID:2MJW) was reported using NMR, mutagenesis and functional assays revealing that the RAGE V binding site in S100P is located in the linker region and in helix-4 and helix-1′ [29]. The residues that showed differential line broadening in the NMR resonances in the HSQC spectrum were clustered in this region. Furthermore, our data from a mutagenesis studies and functional assay showed that the residues E5, D13, F44, Y88 and F89 of S100P play a significant role in RAGE V binding. In the current study, our results indicated that cromolyn binds to the side chains of the hydrophobic residues F44, F89, A84, I81, I12, G9, and M8; the negative amino acid residue at E5 of S100P; and the polar amino acid residue at C85. The binding region of cromolyn (F44, F89, and E5) is involved in the S100P–RAGE V binding interface. The binding constant of S100P–cromolyn ($K_d \sim 181$ μM) was weaker than that of S100P–RAGE V ($K_d \sim 6$ μM). The present study describes the binding properties of S100P–cromolyn and provides knowledge of the binding sites at the molecular level.

Acknowledgments

We sincerely thank the 700 MHz Nuclear Magnetic Resonance Facility in the Department of Chemistry, National Tsing Hua University, Taiwan. We acknowledge financial support from the Ministry of Science and Technology, Taiwan (Grant number: MOST 103-2113-M-007-017-MY3 to Chin Yu) and China Medical University, Taiwan (Grant number: CMU101-N2-04 to Ruey-Hwang Chou).

Appendix A. Supplementary data

Supplementary data associated with this article can be found, in the online version, at http://dx.doi.org/10.1016/j.bbrc.2014.10.048.

References

[1] D.B. Zimmer, P. Wright Sadosky, D.J. Weber, Molecular mechanisms of S100-target protein interactions, Microsc. Res. Tech. 60 (2003) 552–559.
[2] L. Santamaria-Kisiel, A.C. Rintala-Dempsey, G.S. Shaw, Calcium-dependent and -independent interactions of the S100 protein family, Biochem. J. 396 (2006) 201–214.
[3] B.W. Schafer, C.W. Heizmann, The S100 family of EF-hand calcium-binding proteins: functions and pathology, Trends Biochem. Sci. 21 (1996) 134–140.

[4] R. Donato, B.R. Cannon, G. Sorci, F. Riuzzi, K. Hsu, D.J. Weber, C.L. Geczy, Functions of S100 proteins, Curr. Mol. Med. 13 (2013) 24–57.
[5] T. Arumugam, C.D. Logsdon, S100P: a novel therapeutic target for cancer, Amino Acids 41 (2011) 893–899.
[6] E.H. Huang, M.K. Fuentes, T. Arumugam, C.D. Logsdon, The RAGE ligand, S100P, has increased expression in colon cancer, J. Am. Coll. Surg. 199 (2004) S18.
[7] T. Arumugam, D.M. Simeone, A.M. Schmidt, C.D. Logsdon, S100P stimulates cell proliferation and survival via receptor for activated glycation end products (RAGE), J. Biol. Chem. 279 (2004) 5059–5065.
[8] C.W. Heizmann, G.E. Ackermann, A. Galichet, Pathologies involving the S100 proteins and RAGE, Subcell. Biochem. 45 (2007) 93–138.
[9] H.L. Hsieh, B.W. Schafer, B. Weigle, C.W. Heizmann, S100 protein translocation in response to extracellular S100 is mediated by receptor for advanced glycation endproducts in human endothelial cells, Biochem. Biophys. Res. Commun. 316 (2004) 949–959.
[10] M.K. Fuentes, S.S. Nigavekar, T. Arumugam, C.D. Logsdon, A.M. Schmidt, J.C. Park, E.H. Huang, RAGE activation by S100P in colon cancer stimulates growth, migration, and cell signaling pathways, Dis. Colon Rectum 50 (2007) 1230–1240.
[11] J.S.G. Cox, Disodium cromoglycate (Fpl 670) (Intal) – a specific inhibitor of reaginic antibody–antigen mechanisms, Nature 216 (1967) 1328.
[12] W. Storms, M.A. Kaliner, Cromolyn sodium: fitting an old friend into current asthma treatment, J. Asthma 42 (2005) 79–89.
[13] T. Oka, J. Kalesnikoff, P. Starkl, M. Tsai, S.J. Galli, Evidence questioning cromolyn's effectiveness and selectivity as a 'mast cell stabilizer' in mice, Lab. Invest. 92 (2012) 1472–1482.
[14] T. Arumugam, V. Ramachandran, C.D. Logsdon, Effect of cromolyn on S100P interactions with RAGE and pancreatic cancer growth and invasion in mouse models, J. Natl Cancer Inst. 98 (2006) 1806–1818.
[15] T. Arumugam, V. Ramachandran, D. Sun, Z. Peng, A. Pal, D.S. Maxwell, W.G. Bornmann, C.D. Logsdon, Designing and developing S100P inhibitor 5-methyl cromolyn for pancreatic cancer therapy, Mol. Cancer Ther. 12 (2013) 654–662.
[16] S.R. Penumutchu, S.K. Mohan, C. Yu, (1)H, (15)N and (13)C assignments of the calcium bound S100P, Biomol. NMR Assign. 7 (2013) 5–8.
[17] H.A. Benesi, J.H. Hildebrand, A spectrophotometric investigation of the interaction of iodine with aromatic hydrocarbons, J. Am. Chem. Soc. 71 (1949) 2703–2707.
[18] S. Nigam, G. Durocher, Spectral and photophysical studies of inclusion complexes of some neutral 3H-indoles and their cations and anions with beta-cyclodextrin, J. Phys. Chem. 100 (1996) 7135–7142.
[19] S.J. De Vries, M. van Dijk, A.M.J.J. Bonvin, The HADDOCK web server for data-driven biomolecular docking, Nat. Protoc. 5 (2010) 883–897.
[20] T.A. Wassenaar, M. van Dijk, N. Loureiro-Ferreira, G. van der Schot, S.J. de Vries, C. Schmitz, J. van der Zwan, R. Boelens, A. Giachetti, L. Ferella, A. Rosato, I. Bertini, T. Herrmann, H.R.A. Jonker, A. Bagaria, V. Jaravine, P. Guntert, H. Schwalbe, W.F. Vranken, J.F. Doreleijers, G. Vriend, G.W. Vuister, D. Franke, A. Kikhney, D.I. Svergun, R.H. Fogh, J. Ionides, E.D. Laue, C. Spronk, S. Jurksa, M. Verlato, S. Badoer, S. Dal Pra, M. Mazzucato, E. Frizziero, A.M.J.J. Bonvin, WeNMR: structural biology on the grid, J. Grid Comput. 10 (2012) 743–767.
[21] H.M. Zhang, G.Z. Wang, Y. Ding, Z.L. Wang, R. Barraclough, P.S. Rudland, D.G. Fernig, Z.H. Rao, The crystal structure at 2 angstrom resolution of the Ca^{2+}-binding protein S100P, J. Mol. Biol. 325 (2003) 785–794.
[22] S. Hubbard, J.M. Thornton, '{NACCESS}', {C}omputer {P}rogram, {D}epartment of {B}iochemistry and {M}olecular {B}iology, {U}niversity {C}ollege {L}ondon, 1993.
[23] J.P. Linge, M.A. Williams, C.A.E.M. Spronk, A.M.J.J. Bonvin, M. Nilges, Refinement of protein structures in explicit solvent, Proteins 50 (2003) 496–506.
[24] H.J.C. Berendsen, D. Vanderspoel, R. Vandrunen, Gromacs – a message-passing parallel molecular-dynamics implementation, Comput. Phys. Commun. 91 (1995) 43–56.
[25] E. Lindahl, B. Hess, D. van der Spoel, GROMACS 3.0: a package for molecular simulation and trajectory analysis, J. Mol. Model. 7 (2001) 306–317.
[26] A.K. Malde, L. Zuo, M. Breeze, M. Stroet, D. Poger, P.C. Nair, C. Oostenbrink, A.E. Mark, An automated force field topology builder (ATB) and repository: version 1.0, J. Chem. Theory Comput. 7 (2011) 4026–4037.
[27] W. Humphrey, A. Dalke, K. Schulten, VMD: visual molecular dynamics, J. Mol. Graph. Model. 14 (1996) 33–38.
[28] Y. Arendt, A. Bhaumik, R. Del Conte, C. Luchinat, M. Mori, M. Porcu, Fragment docking to S100 proteins reveals a wide diversity of weak interaction sites, ChemMedChem 2 (2007) 1648–1654.
[29] S.R. Penumutchu, R.H. Chou, C. Yu, Structural insights into calcium-bound S100P and the V domain of the RAGE complex, PLoS One 9 (2014).

Supplementary Data

Supplementary Table 1.

List of the active and passive residues used to define the ambiguous interaction restraints for the docking of S100P with cromolyn.

Figure S-1

UV absorption spectra of cromolyn (34 μM) in aqueous buffer solutions.

Figure S-2

Ramachandran map for the S100P-cromolyn complex. The calculations for the plot were performed with the PROCHECK program.

Figure S-3

Molecular dynamics simulation study of the S100P-cromolyn complex. (A) Backbone RMSD plot of the S100P protein, both free and in complex with cromolyn, during the 15 ns molecular dynamics (MD) simulation. Cartoon-stick representations of the S100P-cromolyn complex at 0 ns, 1 ns, 5 ns and 15 ns, as indicated in the figure.

Figure S-4

Far CD measurements of the free S100P and the S100P-cromolyn complex. Secondary structural characterization of wild-type S100P and the S100P-cromolyn complex. The S100P protein and cromolyn were used at a concentration of 10 μM and 350 μM, respectively, in 20 mM Tris (pH 7.0), 100 mM NaCl, and 4 mM $CaCl_2$.

Supplementary Table 1

S100P-Cromolyn Complex	
S100P	
Active Residues	E3, E5, I12, G43, F44, A84, F89,G93
Passive Residues	L4, M10, I11, V14, F15

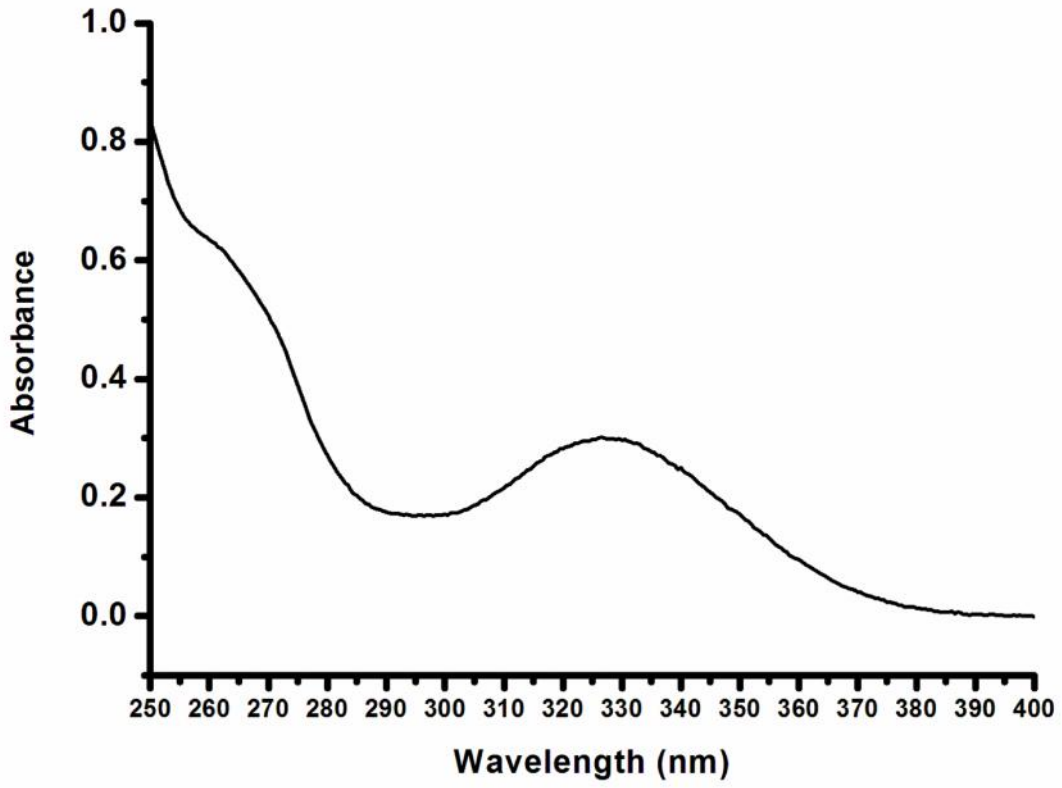

Figure S-1

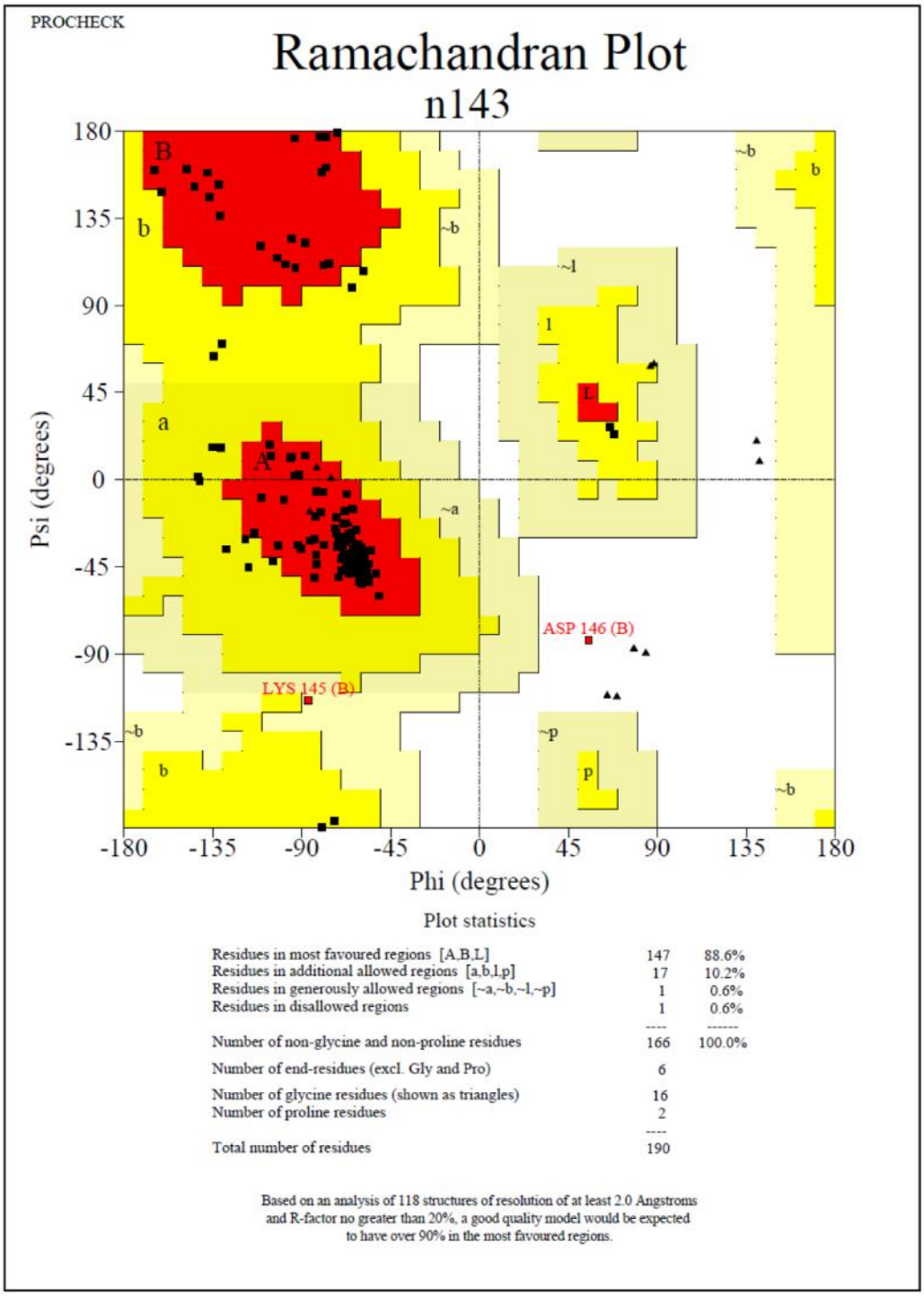
PROCHECK
Ramachandran Plot
n143
Psi (degrees)
Phi (degrees)
ASP 146 (B)
LYS 145 (B)
Plot statistics
Residues in most favoured regions [A,B,L] 147 88.6%
Residues in additional allowed regions [a,b,l,p] 17 10.2%
Residues in generously allowed regions [~a,~b,~l,~p] 1 0.6%
Residues in disallowed regions 1 0.6%
Number of non-glycine and non-proline residues 166 100.0%
Number of end-residues (excl. Gly and Pro) 6
Number of glycine residues (shown as triangles) 16
Number of proline residues 2
Total number of residues 190
Based on an analysis of 118 structures of resolution of at least 2.0 Angstroms
and R-factor no greater than 20%, a good quality model would be expected
to have over 90% in the most favoured regions.

Figure S-2

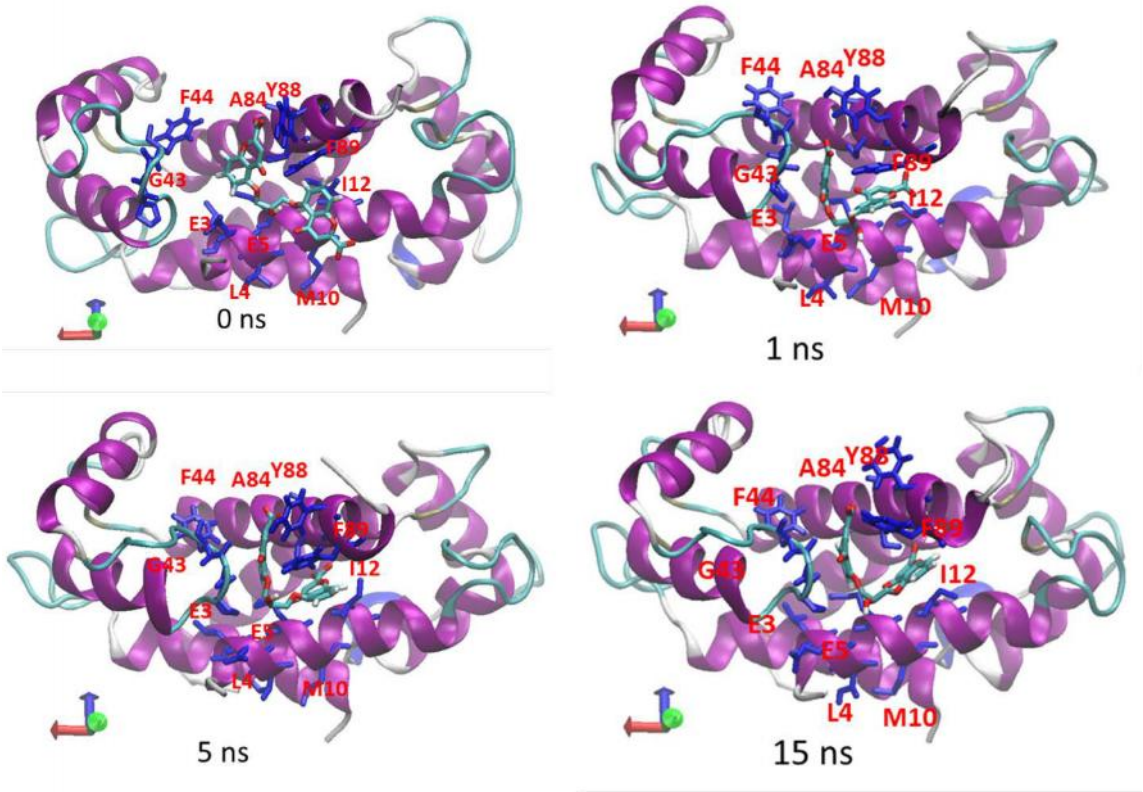

Figure S-3

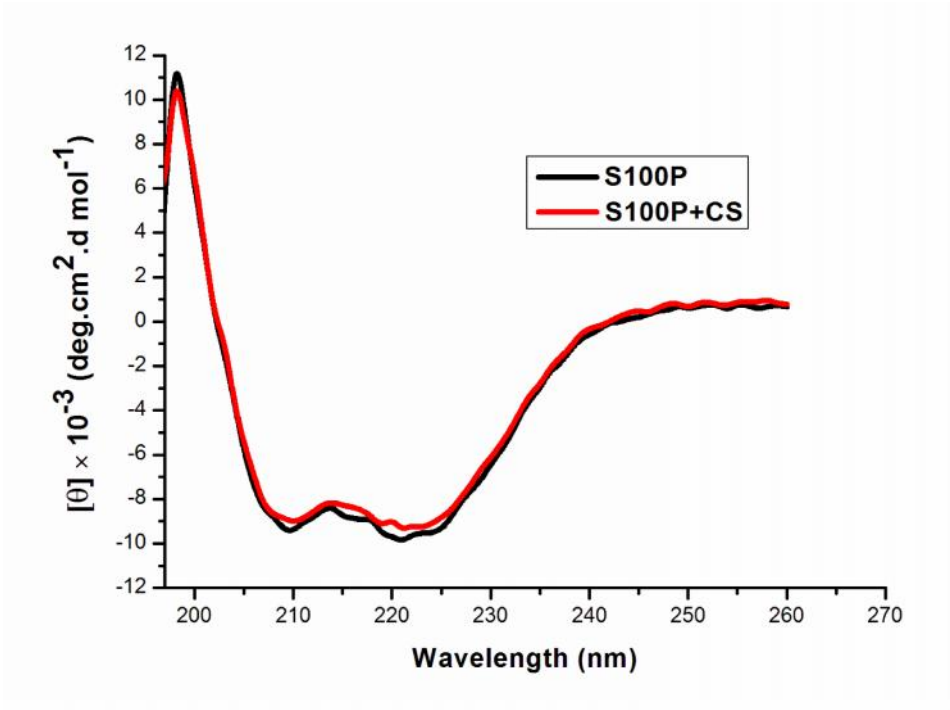

Figure S-4